nature medicine

Reducing endoplasmic reticulum stress through a macrophage lipid chaperone alleviates atherosclerosis

Ebru Erbay[1], Vladimir R Babaev[2], Jared R Mayers[1], Liza Makowski[3], Khanichi N Charles[1], Melinda E Snitow[1], Sergio Fazio[2], Michelle M Wiest[4], Steven M Watkins[4], MacRae F Linton[2] & Gökhan S Hotamisligil[1]

Macrophages show endoplasmic reticulum (ER) stress when exposed to lipotoxic signals associated with atherosclerosis, although the pathophysiological importance and the underlying mechanisms of this phenomenon remain unknown. Here we show that mitigation of ER stress with a chemical chaperone results in marked protection against lipotoxic death in macrophages and prevents macrophage fatty acid–binding protein-4 (aP2) expression. Using genetic and chemical models, we show that aP2 is the predominant regulator of lipid-induced macrophage ER stress. The absence of lipid chaperones incites an increase in the production of phospholipids rich in monounsaturated fatty acids and bioactive lipids that render macrophages resistant to lipid-induced ER stress. Furthermore, the impact of aP2 on macrophage lipid metabolism and the ER stress response is mediated by upregulation of key lipogenic enzymes by the liver X receptor. Our results demonstrate the central role for lipid chaperones in regulating ER homeostasis in macrophages in atherosclerosis and show that ER responses can be modified, genetically or chemically, to protect the organism against the deleterious effects of hyperlipidemia.

Organelle-mediated stress, particularly ER stress, has recently emerged as a major pathophysiological paradigm underlying chronic metabolic diseases[1–8]. In conjunction with its central role in protein synthesis, folding and transportation, the ER serves as a key site for integrating cellular responses to stress[9]. The presence of misfolded proteins and other stresses lead to the activation of an adaptive program by the ER, known as the unfolded protein response (UPR), to reestablish equilibrium[9]. Initiation of the canonical UPR engages three distinct signaling branches mediated by pancreatic ER kinase (PERK), inositol-requiring transmembrane kinase/endonuclease-1 (IRE-1) and activating transcription factor-6 (ATF6). The UPR is also linked to the activation of stress kinases such as the c-Jun N-terminal kinase (JNK). The combined action of these pathways leads to inhibition of protein translation, stimulation of protein degradation and production of chaperone proteins, resulting in either recovery of ER function or cell death[10].

In obesity, activation of the UPR in metabolic tissue contributes to insulin resistance, at least in part through IRE-1–dependent, JNK-1–mediated inhibition of insulin action[5]. Promotion of ER stress by genetic haploinsufficiency of X box–binding protein-1 (XBP-1), which functions in the UPR-induced transcriptional program, also leads to systemic insulin resistance, whereas alleviation of ER stress by chemical or molecular chaperones, small compounds or proteins that facilitate proper protein folding and stability, protects mice against insulin resistance and type 2 diabetes[5–7]. Activation of the ER stress response pathways is also a characteristic of lipid-laden macrophages in atherosclerotic lesions in mice and humans and is proposed to have a role in plaque vulnerability and acute cardiac death[3,4,8]. However, the role of ER stress in macrophages and cardiovascular disease remains obscure, and it is unknown whether the modulation of ER stress pathways can alter the function and survival of macrophages and the course of atherosclerosis. Moreover, it is unclear how accumulation of excess lipids in macrophages can engage the ER stress response pathways. Despite continuing debate, it is likely that the biological effects of toxic lipids, such as those prevalent in dyslipidemia, are signaled through specific pathways rather than through the nonspecific demise of cellular function and viability that occurs during lipotoxicity. Several pieces of evidence suggest a connection between lipid metabolism and the UPR. For example, XBP-1 has a role in ER phosphatidylcholine synthesis and endomembrane expansion and has been linked to transcriptional regulation of several lipogenic genes in the liver[11,12]. ER stress can induce lipogenesis and promote hepatic steatosis[12–15]. In contrast, inhibition of phospholipid synthesis or increasing phospholipase activity exacerbates ER stress responses, and sphingolipid levels can influence ER function[16,17]. Additionally, ER stress has been identified as a mechanism driving free cholesterol–induced cell death in a model of cholesterol loading[3]. Hence, it is possible that the ER may serve as a major target organelle that senses stresses related to lipid status and exposure[10]. However, the signaling networks linking ER function, lipid metabolism and the physiological outcomes are not known.

Cellular lipid metabolism and reception of lipid signals are regulated by cytosolic lipid chaperones, particularly aP2, which have profound effects on chronic metabolic diseases and whose function is relevant to human disease[10,18–23]. The dramatic impact of aP2 on atherosclerosis is related exclusively to its action in the macrophages,

[1]Department of Genetics & Complex Diseases, Harvard School of Public Health, Boston, Massachusetts, USA. [2]Department of Medicine, Vanderbilt University, Nashville, Tennessee, USA. [3]Duke University Medical Center, Sarah W. Stedman Nutrition Center, Chapel Hill, North Carolina, USA. [4]Lipomics Technologies, West Sacramento, California, USA. Correspondence should be addressed to G.S.H. (ghotamis@hsph.harvard.edu).

Received 27 July; accepted 31 October; published online 29 November 2009; corrected after print 4 February 2010; doi:10.1038/nm.2067

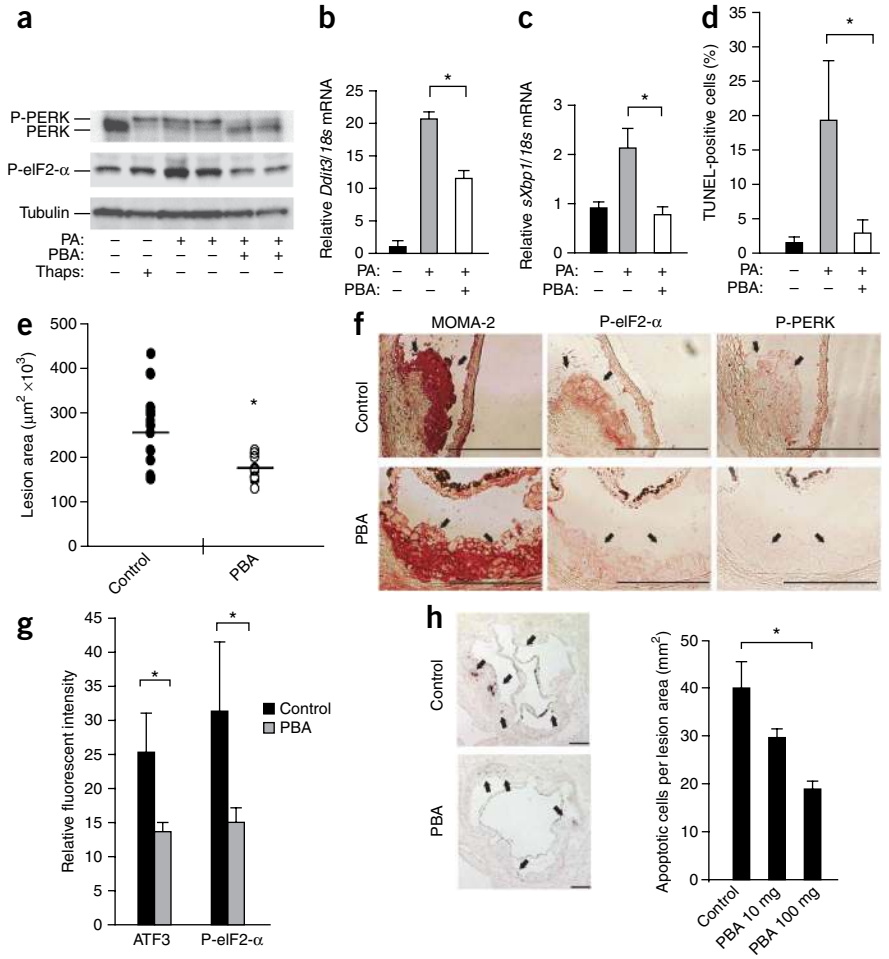

Figure 1 PBA treatment protects against macrophage ER stress and reduces vascular disease progression. (**a**) P-PERK and P-eIF2-α, as determined by western blotting, (**b**,**c**) mRNA levels of *Ddit3* and s*Xbp1*, respectively, as determined by quantitative RT-PCR (qRT-PCR), and (**d**) apoptosis, as determined by TUNEL assays, in WT macrophages after ER stress induced by 500 μM palmitate (PA) or 300 nM thapsigargin (Thaps) in the presence or absence of 3 mM PBA. Data represent means ± s.e.m.; * $P < 0.05$. (**e**) Atherosclerotic lesion area in the aortic sinus from mice treated with either control or PBA (100 mg per kg body weight) for 2 weeks ($n \geq 13$). Data represent means ± s.d.; * $P < 0.05$. (**f**) Serial immunohistological sections stained with antibodies against P-PERK, P-eIF2-α and MOMA-2. Red indicates positive staining with antibody. Scale bars, 200 μm. (**g**) Relative fluorescent intensity for antibody staining corresponding to ATF3 and P- eIF2-α expression ($n \geq 3$) in the macrophage-dense areas in **Supplementary Figure 1g**. Data represent means ± s.d.; * $P < 0.05$. (**h**) Left apoptotic cells (TUNEL-positive) in the aortic sinus area are shown for PBS- (control) or 100 mg per kg body weight PBA-treated (PBA) mice. Arrows point to apoptotic cells. Scale bars, 200 μm. Right, percentage of apoptotic cells in the aortic sinus area, shown in PBS-treated (Control), 10 mg per kg body weight PBA-treated (PBA 10 mg) or 100 mg per kg body weight PBA-treated (PBA 100 mg) mice. *$P < 0.05$.

although the underlying mechanisms are not fully resolved[22]. The fact that macrophage aP2 deficiency can mediate protection from atherosclerosis in the setting of severe dyslipidemia has raised the possibility that lipid chaperones may be a link between toxic lipids and organelle stress in macrophages.

Here we explored the mechanisms related to lipotoxic macrophage ER stress and the impact of ER dysfunction on atherosclerosis using a chemical chaperone and lipid chaperone–deficient mouse model. We show that mitigation of ER stress is protective against atherosclerosis and that aP2 is an obligatory intermediate for macrophage ER stress responses to lipids.

RESULTS

Blocking macrophage ER stress and atherosclerosis

The chemical chaperone 4-phenyl butyric acid (PBA) can alleviate ER stress and, hence, provides an experimental opportunity to approach the role of ER stress in atherosclerosis[7,24]. We first tested whether PBA can alter ER stress induced in macrophages upon exposure to saturated fatty acids[25,26]. Treatment with palmitate induced ER stress in macrophages, as determined by phosphorylation of PERK (P-PERK) and eukaryotic translation initiation factor 2α (P-eIF2-α) (**Fig. 1a**). However, concurrent treatment with PBA resulted in essentially complete protection against palmitate-induced ER stress (**Fig. 1a**). PBA treatment also suppressed palmitate-induced splicing of XBP-1 (sXBP-1) and C/EBP homologous protein expression (CHOP, which is encoded by *Ddit3*), two elements of the UPR-induced transcriptional program (**Fig. 1b**,**c**). Because saturated fatty acids or modified lipoproteins can induce apoptotic pathways, we next asked whether modifying ER stress in this setting could prevent lipotoxic death in macrophages[27]. Treatment with PBA resulted in marked protection against palmitate-induced apoptosis in macrophages, as determined by TUNEL assays (**Fig. 1d** and **Supplementary Fig. 1a**). These results show that PBA can protect cultured macrophages against lipid-induced ER stress and apoptosis *in vitro*.

Next, to elucidate whether PBA can mitigate ER stress in atherosclerotic lesions *in vivo*, we analyzed ER stress indicators and apoptosis in serial sections from aortic sinuses of atherosclerotic mice briefly treated with PBA. We fed 6-week-old, male, apolipoprotein E–deficient (*Apoe*)$^{-/-}$ mice with a Western diet for 8 weeks and gave them daily doses (10 mg per kg body weight or 100 mg per kg body weight) of PBA or vehicle during the final 2 weeks. Examination of the sections of the aortic sinus for proximal lesions indicated that *Apoe*$^{-/-}$ mice receiving PBA showed a dose-dependent reduction (9% at 10 mg per kg body weight, not significant, and 32% at 100 mg per kg body weight, $P < 0.05$) in atherosclerosis (**Fig. 1e** and data not shown). At this early stage of atherosclerosis, *en face* analysis was similar between the groups (**Supplementary Fig. 1b**). Of note, suppression of macrophage ER stress and reduction in vascular lesions by PBA treatment occurred in the absence of any impact on lipids, lipoprotein profiles, glucose and insulin levels in the circulation (**Supplementary Fig. 1c–f** and data not shown) and on body weight (30.6 ± 0.4 g versus 29.5 ± 0.6 g; $P = 0.19$).

Hence, this relatively short treatment period provided a suitable experimental design to examine the status of ER stress indicators and apoptosis in atherosclerotic lesions without substantial changes in systemic metabolic parameters, insulin sensitivity or the

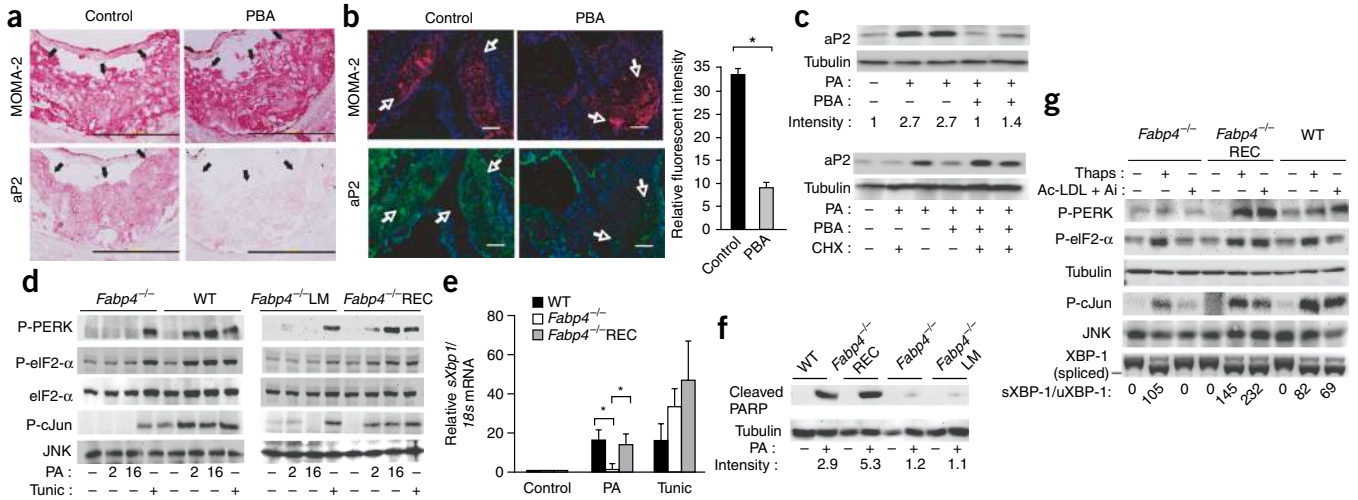

Figure 2 Requirement for aP2 in lipid-induced ER stress and apoptosis. (**a**,**b**) Serial sections from aortic sinus of PBS-(control) or PBA-treated *Apoe*$^{-/-}$ mice stained with antibodies against MOMA-2 or aP2. Arrows point to red staining for these antibodies in macrophage-dense areas. Scale bars: 200 μm in **a**, 100 μm in **b**. Relative fluorescence intensity for aP2 expression (green) in the macrophage-dense areas (red) of the lesions is shown in **b**. Data represent means ± s.d.; $*P < 0.05$ and $n \geq 3$. (**c**) aP2 expression, as determined by western blotting, in palmitate (500 μM)-treated macrophages in the presence or absence of 3 μM PBA or 100 μg ml^{-1} cycloheximide (CHX). Relative band intensity is reported as the ratio of the band intensity for aP2 in the treated sample to that in the untreated sample. (**d**) P-PERK and P-eIF2-α abundance, as examined by western blotting, and JNK activity (P-cJun), as determined by an *in vitro* kinase assay, from 500 μM palmitate–treated (2 or 16 h) macrophages. (**e**) s*Xbp1* expression, as examined by qRT-PCR in (500 μM) palmitate–treated or (2 μg ml^{-1}) tunicamycin (Tunic)-treated (12 h) macrophages. Data represent means ± s.d.; $*P < 0.05$ and $n \geq 3$. (**f**) Cleaved PARP and tubulin expression, as examined by western blotting, in palmitate-treated (24 h) macrophages. Relative band intensities were quantified, and data represent means ± s.e.m.; $*P < 0.05$. (**g**) P-PERK and P-eIF2-α expression, as examined by western blotting, and JNK activity (P-c-Jun), as determined by a kinase assay, and s*Xbp1* (unspliced, top band; spliced, bottom band), as determined by RT-PCR, from macrophages treated with 10 μM ACAT inhibitor (Ai) and 100 μg ml^{-1} acetylated low-density lipoprotein (Ac-LDL) (24 h) or 300 nM thapsgiargin (Thaps). The ratio of relative intensities corresponding to spliced (s*Xbp1*) and unspliced (u*Xbp1*) were calculated.

total burden of lesions that occurs with longer PBA treatment (data not shown)[7,24]. Immunohistochemical analysis revealed that all mice developed early lesions that predominantly contained macrophages and macrophage-derived foam cells (shown by staining with monocytes and macrophage–specific antibody, MOMA-2) (**Fig. 1f**). There was no significant reduction in total macrophage area upon PBA treatment, despite a reduction in lesion size (macrophage area in control, 123,097 ± 13,711 μm^2 in PBA treatment, 170,545 ± 30,249 μm^2). The atherosclerotic lesions of *Apoe*$^{-/-}$ (control) mice stained positively for the ER stress markers P-eIF2-α and P-PERK in macrophage-dense areas (**Fig. 1f**). In contrast, P-eIF2-α and P-PERK staining was markedly diminished in atherosclerotic lesions of mice treated with PBA (**Fig. 1f**). Immunofluorescence staining revealed a 44% reduction in activating transcription factor-3 (ATF3), a cyclic AMP–dependent transcription factor that is induced by ER stress, expression ($P < 0.05$) and a 53% reduction in P-eIF2-α expression ($P < 0.05$) in the macrophage-dense areas of the lesions after PBA treatment (**Fig. 1g** and **Supplementary Fig. 1g**). We also examined the extent of apoptosis in these atherosclerotic lesions by TUNEL staining. Atherosclerotic lesions from control mice contained abundant apoptotic cells, whereas lesions from PBA-treated mice showed a significant reduction in apoptotic cells in a dose-dependent manner (29% at 10 mg per kg body weight and 42% at 100 mg per kg body weight; $P < 0.05$ in the 100 mg per kg body weight dose) (**Fig. 1h**). These results show that PBA treatment leads to a marked reduction in macrophage ER stress and apoptosis in atherosclerotic lesions *in vivo*, indicating that improvement of ER chaperoning function can protect against the deleterious effects of toxic lipids in promoting atherosclerotic lesions.

Regulation of lipid-induced ER stress by a lipid chaperone

It has been shown that aP2 deficiency in macrophages protects against atherosclerosis, despite a highly unfavorable lipid profile[22,28,29]. Because toxic lipids fail to trigger ER stress in the presence of PBA, we investigated whether lipid chaperoning activity is linked to ER stress and PBA activity in macrophages. Notably, aP2 immunostaining was significantly suppressed in vascular lesions of *Apoe*$^{-/-}$ mice treated with PBA when compared to vehicle-treated (control) mice (71%, $P < 0.05$) (**Fig. 2a**,**b**). Furthermore, palmitate induced rapid and marked upregulation of aP2 protein levels but not *Fabp4* (encoding aP2) messenger RNA levels (**Fig. 2c** and **Supplementary Fig. 2a**). Induction of aP2 by palmitate was prevented upon concurrent treatment with PBA (**Fig. 2c** and **Supplementary Fig. 2a**). Taken together, these results indicate that aP2 expression is directly related to lipid-induced ER stress and is strongly inhibited by PBA in macrophages *in vitro* and *in vivo*. This observation led us to ask whether aP2 regulates ER responses to lipid stress in macrophages. Treatment of wild-type (WT) macrophages with long-chain saturated fatty acids such as palmitate or stearate, but not their monounsaturated counterparts, led to ER stress, as judged by the robust phosphorylation of PERK and eIF2-α, activation of JNK and induction DNA damage–inducible transcript-3 (*Ddit3*) and s*Xbp1* expression (**Fig. 2d**,**e** and **Supplementary Fig. 2b**,**d**,**g**). However, palmitate failed to induce ER stress in aP2-deficient (*Fabp4*$^{-/-}$) macrophages (**Fig. 2d**,**e** and **Supplementary Fig. 2g**). In these cell lines, there were no alterations in palmitate uptake (**Supplementary Fig. 2e**). The *Fabp4*$^{-/-}$ cells also maintained the ability to respond to tunicamycin, an inhibitor of protein glycosylation that leads to ER stress, indicating that they do not suffer from a general defect in mounting ER stress responses (**Fig. 2d**,**e**).

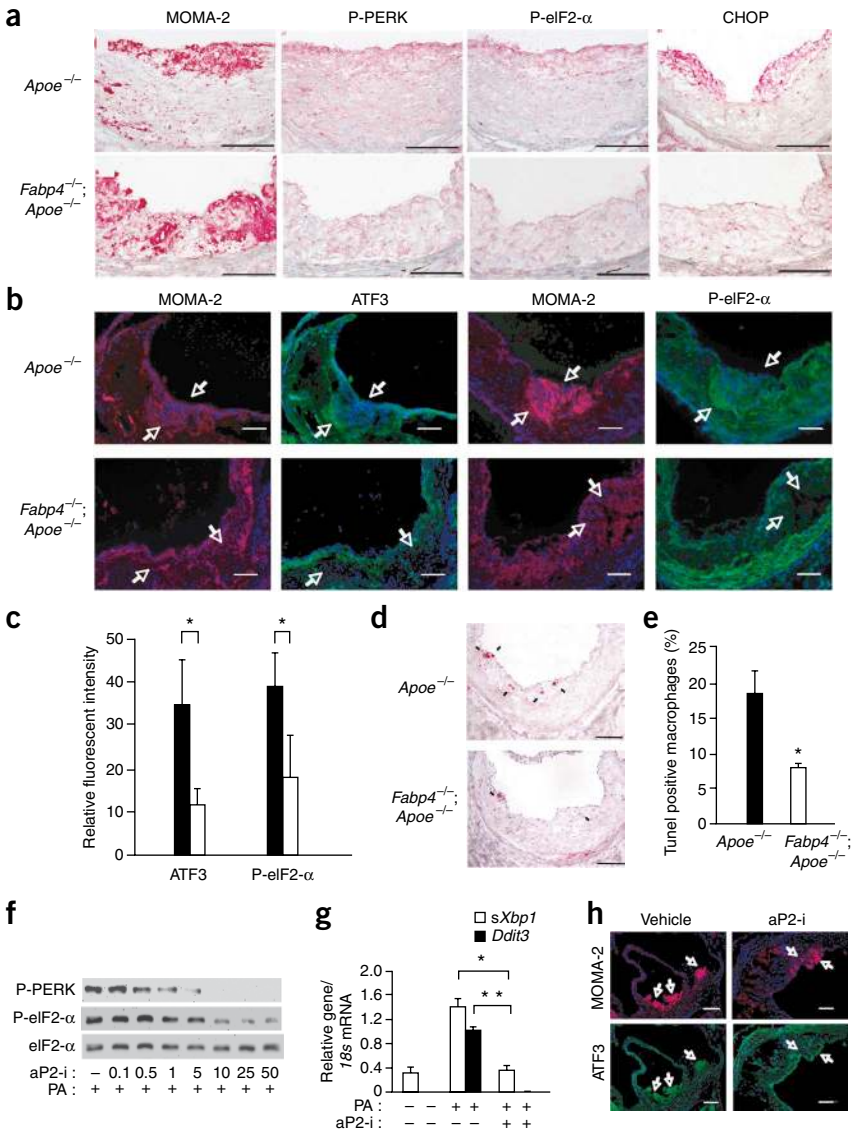

Figure 3 aP2 deficiency protects from hypercholesteremia-induced macrophage ER stress and apoptosis in atherosclerotic lesions. (**a**,**b**) Immunohistochemical staining with antibodies against MOMA-2, P-PERK and P-eIF2-α (**a**,**b**), CHOP (**a**) and ATF3 (**b**) in atherosclerotic lesions from the proximal aorta of *Apoe*$^{-/-}$ and *Fabp4*$^{-/-}$;*Apoe*$^{-/-}$ mice fed a Western diet for 16 weeks. Arrows point to ATF3 and P-eIF2-α (green), expressed in the MOMA-2–positive (red) areas of the lesions. Scale bars: in **a**, 50 μm; in **b**, 100 μm. (**c**) Relative fluorescent intensity for stainings corresponding to ATF3 and P-eIF2-α in the macrophage-dense areas. Data represent means ± s.d.; $*P < 0.05$, $n \geq 3$. (**d**,**e**) Apoptotic macrophages in the lesions from *Apoe*$^{-/-}$ and *Fabp4*$^{-/-}$;*Apoe*$^{-/-}$ mice, as determined by TUNEL assay. A typical micrograph from each strain is shown (**d**) along with quantification (**e**). Arrows point to apoptotic cells. Scale bars, 100 μm. $*P < 0.05$. (**f**,**g**) P-PERK and P-eIF2-α abudance (**f**), determined by western blotting, and s*Xbp1* and *Ddit3* mRNA levels (**g**), analyzed by qRT-PCR, from macrophages treated with 25 μM of aP2-i in macrophage lines stressed with palmitate (500 μM) in the presence of vehicle (–) or varying doses of aP2-i (0.1-50 μM). (**h**) Double immunofluorescent staining with antibodies against MOMA-2 and ATF3 in the atherosclerotic lesions from *Apoe*$^{-/-}$ mice treated with vehicle or aP2-i (15 mg per kg body weight for 14 weeks). Arrows indicate staining for ATF3 (green) in MOMA-2–positive areas (red). Scale bars, 100 μm.

We then compared ER stress responses in *Fabp4*$^{-/-}$ macrophages reconstituted with a lipid-binding mutant (LM) of aP2 (R126L, Y128F; *Fabp4*$^{-/-}$LM) to those reconstituted with WT aP2 (*Fabp4*$^{-/-}$REC)[30]. Under the conditions tested, WT- and LM-aP2 proteins were expressed in comparable amounts and did not lead to any alterations in lipid uptake (**Supplementary Fig. 2e** and data not shown). Reconstitution of WT-aP2 rendered *Fabp4*$^{-/-}$ macrophages responsive to palmitate, as indicated by the induction of P-PERK, P-eIF2-α and JNK activity, whereas *Fabp4*$^{-/-}$LM macrophages remained markedly resistant to palmitate-induced ER stress (**Fig. 2d**). Palmitate also induced the expression of *Ddit3* and s*Xbp1* in WT but not in *Fabp4*$^{-/-}$ macrophages (**Supplementary Fig. 2g** and **Fig. 2e**). In *Fabp4*$^{-/-}$ macrophages, reconstitution of aP2 restored the induction of UPR target genes by palmitate (**Fig. 2d**,**e** and **Supplementary Fig. 2g**). Consistent with their ER stress–resistant phenotype, *Fabp4*$^{-/-}$ macrophages were also significantly protected against palmitate-induced apoptosis, as indicated by suppression of caspase-3 activity and poly–ADP-ribose polymerase (PARP) cleavage (**Fig. 2f** and **Supplementary Fig. 2h**). Reconstitution of WT-aP2 into the *Fabp4*$^{-/-}$ macrophages rendered these cells susceptible to lipid-induced apoptosis, whereas cells expressing LM-aP2 remained refractory to apoptosis, showing the requirement for the lipid-binding activity of aP2 in regulating ER stress responses (**Fig. 2f** and **Supplementary Fig. 2h**).

Next, we exposed macrophages to free cholesterol loading to examine ER stress responses in another setting of lipotoxicity associated with the pathogenesis of atherosclerosis[4]. In WT, but not *Fabp4*$^{-/-}$, macrophages, free cholesterol induced ER stress, as indicated by the induction of phosphorylation of PERK and eIF2-α, sXBP-1 mRNA expression and JNK activity (**Fig. 2g**). These observations were also independent of compromised cholesterol uptake; in fact, *Fabp4*$^{-/-}$ macrophages show increased cholesterol influx[31]. Responsiveness to free cholesterol–induced ER stress was restored in *Fabp4*$^{-/-}$ macrophages upon reconstitution of aP2, indicating that aP2 mediates free cholesterol–induced ER stress in macrophages (**Fig. 2g**). Furthermore, *Fabp4*$^{-/-}$ macrophages were resistant to free cholesterol–induced apoptosis, as determined by activation of caspase-3 and cleavage of PARP, which normally occurs in free cholesterol–treated WT macrophages (**Supplementary Fig. 2i**)[3]. Taken together, our results show that aP2 is necessary for toxic lipids to trigger ER stress and apoptosis in macrophages.

Regulation of macrophage ER stress by aP2 *in vivo*

We next investigated whether aP2 deficiency in mice can modulate ER stress responses in vascular lesions *in vivo*. The *Fabp4*$^{-/-}$ mouse model provides an ideal setting to examine the link between

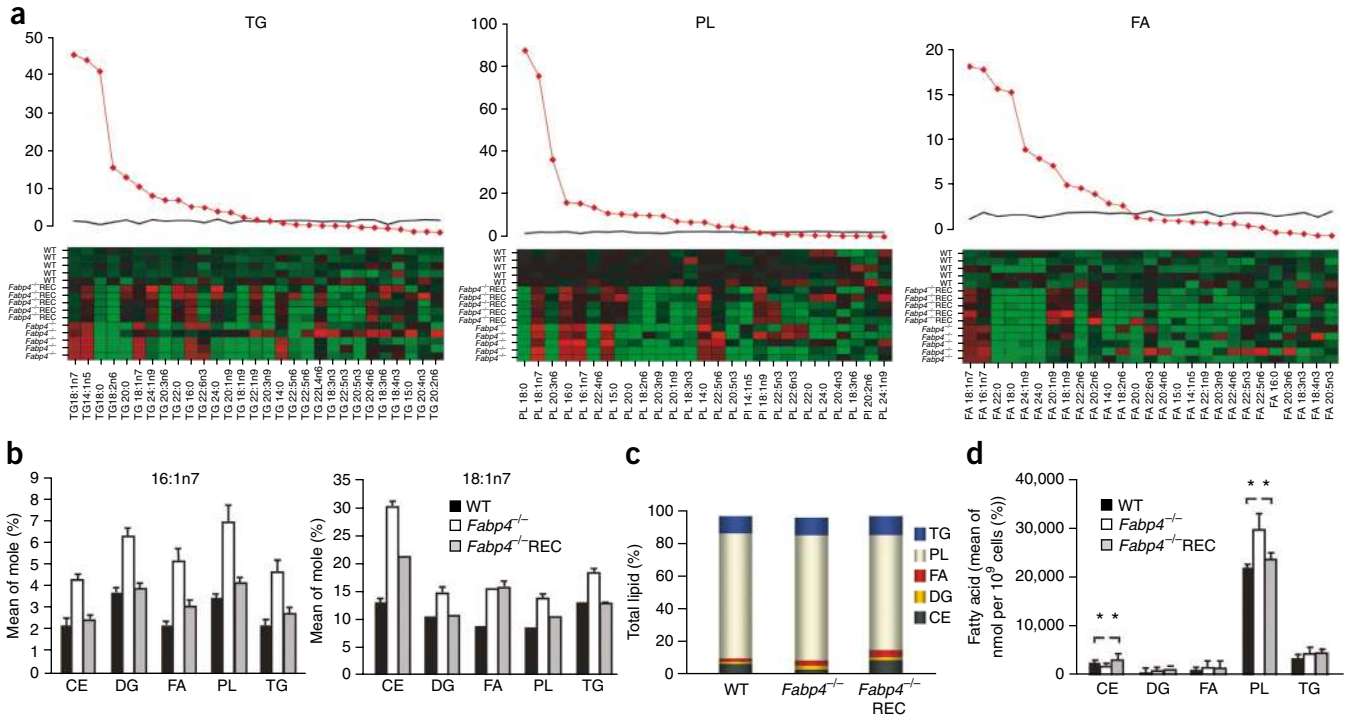

Figure 4 Regulation of macrophage lipid composition by aP2. (**a**) Lipid class composition analysis for triglycerides (TG), phospholipids (PL) and fatty acids (FA). The F statistics from one-way analysis of variance (ANOVA) are shown as red diamonds over the distribution of F statistics from permuted data. The black line is the 95th percentile of the F statistics over 1,000 permutations. The higher the value of the F statistics from ANOVA, the more different the groups are. The heat map shows the observed data centered to the mean of the WT genotype and scaled by the s.d. of all observations. (**b**) The mean concentration (mole (%); the ratio of moles of fatty acids to total moles of fatty acid in each lipid class) of C16:1n7 and C18:1n7 for each lipid class in the various macrophage lines.(**c**,**d**) Percentage total lipids (**c**) and bar plots of the mean concentration of lipids (**d**) in the macrophage lines. Data represent means ± s.d.; $^*P < 0.05$ and $n \geq 3$.

macrophage ER stress and atherosclerosis, as aP2 deficiency does not alter the hyperlipidemia or any other metabolic parameters in the *Apoe*$^{-/-}$ background, and, furthermore, the impact of aP2 on atherosclerosis is predominantly, if not completely, mediated by its action in the macrophages[22]. The early-stage atherosclerotic plaques from *Apoe*$^{-/-}$ mice showed induction of ER stress, as indicated by elevated PERK and eIF2-α phosphorylation and CHOP levels in the infiltrating macrophages within the lesions (**Fig. 3a**). Notably, the vascular lesions in the *Fabp4*$^{-/-}$; *Apoe*$^{-/-}$ mice were essentially devoid of staining for markers of ER stress (**Fig. 3a**). Quantitative analysis of ER stress by immunofluorescent staining showed a significant reduction in P-eIF2-α and ATF3 (55% and 67%, respectively; $P < 0.05$) expression in macrophage-rich areas of the lesions (**Fig. 3b**,**c**). Furthermore, TUNEL assays showed a significant reduction in the number of apoptotic macrophages in lesions of *Fabp4*$^{-/-}$;*Apoe*$^{-/-}$ mice compared to *Apoe*$^{-/-}$ mice (7.8% and 18.4%, respectively; $P < 0.05$) (**Fig. 3d**,**e** and **Supplementary Fig. 3a**). This confirmed the crucial role of aP2 in mediating macrophage ER stress response to toxic lipids *in vivo,* similar to its actions in cultured macrophages *in vitro*.

The impact of genetic aP2 deficiency can be mimicked by a specific chemical inhibitor for aP2 (aP2-i) *in vitro* and *in vivo*[29]. Treatment of WT macrophages with aP2-i also led to marked protection against palmitate-induced ER stress, as assessed by diminished P-PERK and P-eIF2-α abundance and *Ddit3* and s*Xbp1* expression, without any effects on fatty acid uptake (**Fig. 3f**,**g** and **Supplementary Fig. 3b**). Treatment with aP2-i also lowered ATF3 expression in macrophage-dense areas of the plaques in *Apoe*$^{-/-}$ mice *in vivo*, without altering hyperlipidemia (**Fig. 3h**)[29]. These results clearly show that genetic or chemical ablation of aP2 protects macrophages from ER stress *in vivo* in the context of hypercholesterolemic atherosclerosis.

Mechanisms linking aP2 to macrophage ER stress

To identify the metabolic pathways that control the observed tolerance to toxic lipids, we next studied the impact of aP2 on macrophage lipid composition and metabolism. We analyzed the profiles of individual fatty acids in macrophages in a systematic manner using high-resolution, quantitative lipidomic analysis. *Fabp4*$^{-/-}$ macrophages contained elevated levels of monounsaturated fatty acids (MUFAs), indicating that a greater proportion of the lipids in these cells were produced *de novo* (**Supplementary Table 1**). Furthermore, we saw evidence of increased steaoryl CoA desaturase (SCD) activity in *Fabp4*$^{-/-}$ macrophages, reflected in the elevated C16:1n7/C16:0; C14:1n5/C14:0, and C18:1n9/C18:0 ratios of fatty acids present in various lipid classes (**Fig. 4a** and **Supplementary Table 1**). Enhancement of *de novo* lipogenesis in *Fabp4*$^{-/-}$ macrophages resulted in a marked increase in the abundance of C16:1n7 and its direct elongation product, C18:1n7, in addition to a modest elevation in C14:1n5 and C18:1n9 (**Fig. 4b** and **Supplementary Table 1**). The reconstitution of aP2 markedly shifted the fatty acid profile from one of active *de novo* synthesis, with enhanced desaturase activity, to high elongase activity with little desaturase action, indicating that macrophage *de novo* lipogenesis is strongly regulated by aP2 (**Fig. 4a**,**b**).

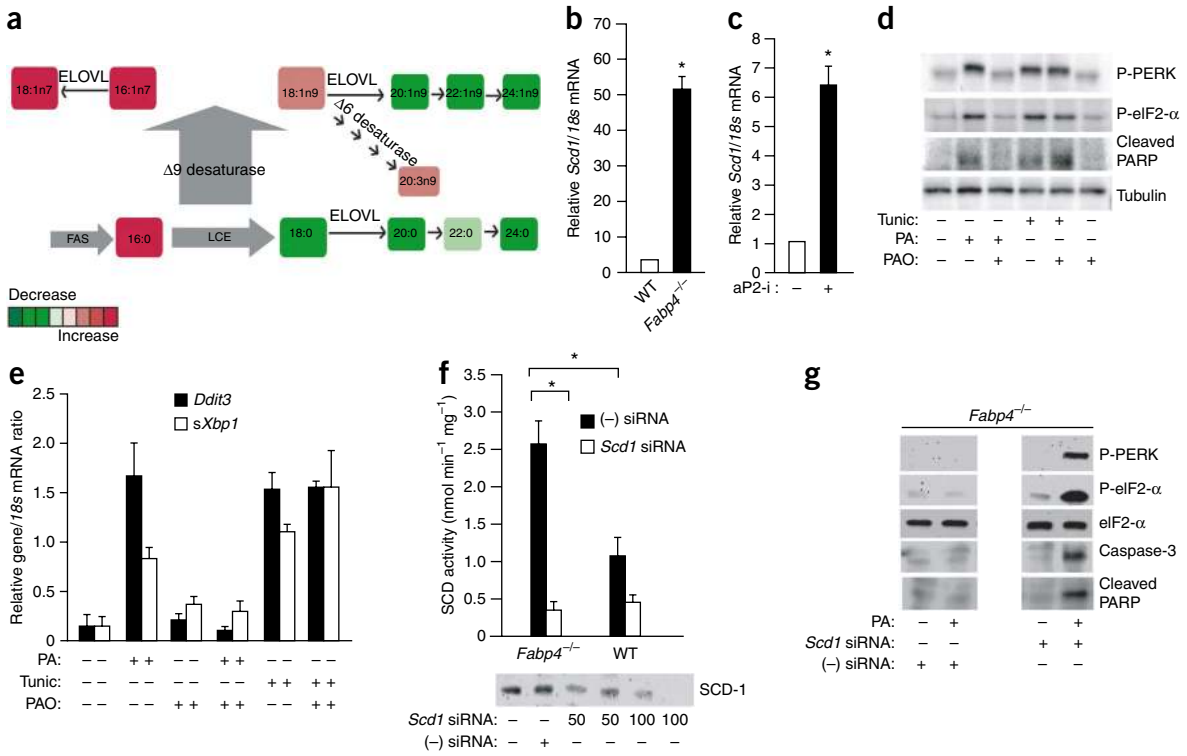

Figure 5 A central role for SCD and C16:1n7 in aP2 mediated lipotoxic signaling. (**a**) A summary of the lipid changes that occur as a result of aP2 deficiency in macrophages. LCE, fatty acid long chain elongase; ELOVL, fatty acid elongase for very long chain fatty acid. (**b**,**c**) *Scd1* mRNA levels, as determined by qRT-PCR in primary peritoneal macrophages at the base line (**b**) or after treatment of mice with aP2-i for 6 weeks ($n = 6$) (**c**). Data represent means ± s.e.m.; $^*P < 0.05$. (**d**,**e**) P-PERK, P-eIF2-α and cleaved PARP abundance (**d**), examined by western blotting, and *Ddit3* and s*Xbp1* mRNA levels (**e**), examined by qRT-PCR. ER stress was induced in macrophages by palmitate (300 μM) or tunicamycin (2 mM) treatment. Cells were pretreated with palmitoleate (PAO) (300 μM) where indicated. (**f**) SCD activity (top), examined by an enzymatic assay, and SCD protein expression (bottom), as examined by western blotting, from macrophage lines treated with *Scd1*-specific siRNA (50–100 nM) or scrambled (–) siRNA. Data represent means ± s.e.m.; $^*P < 0.05$. (**g**) P-PERK, P-eIF2-α and cleaved PARP abundance, examined by western blotting from lysates of *Fabp4*$^{-/-}$ macrophages treated with negative (–) siRNA or *Scd1*-specific siRNA (100 nM) and treated with or without palmitate (500 μM).

We next asked which lipid classes are enriched by these newly synthesized fatty acids and determined the distribution of all major classes of lipids. When compared to WT macrophages, *Fabp4*$^{-/-}$ macrophages had elevated phospholipids (138%), triglycerides (140%), diacylglycerol (143%) and free fatty acid (224%) concentrations and lower levels of cholesterol esters (79%) (**Fig. 4c**,**d**). Reconstitution of aP2 suppressed phospholipid levels by 31% and markedly increased cholesterol ester concentrations by 197%, demonstrating a crucial role for aP2 in the regulation of macrophage phospholipid and cholesterol production (**Fig. 4c**,**d**). The marked increase in the phospholipid-to-cholesterol ratio seen in the *Fabp4*$^{-/-}$ macrophages suggests that one potential way aP2 can modulate stress responses to toxic lipids may be through alteration in membrane lipid composition and metabolic properties.

The results of lipidomic analysis implicated regulation of *de novo* lipogenesis and desaturation, a rate-limiting step catalyzed by SCD, as a potential mechanism underlying the aP2-driven compositional changes in macrophages (**Fig. 5a**). The desaturase activity of SCD converts saturated fatty acids to MUFAs, which are then incorporated into phospholipids, triglycerides and cholesterol esters[32,33]. Indeed, *Fabp4*$^{-/-}$ macrophages are enriched with MUFAs, most substantially in C16:1n7-palmitoleate and its direct elongation product, C18:1n7, across all major lipid classes (**Fig. 4b** and **Supplementary Table 1**). Consistently, SCD-1 expression in *Fabp4*$^{-/-}$ macrophages was ~50-fold higher than that in WT controls (**Fig. 5b**). Next, we examined aP2-regulated SCD-1 expression in macrophages *in vivo* and found that its expression was markedly upregulated in the peritoneal macrophages isolated from mice treated with aP2-i (**Fig. 5c**). Fatty acid synthase (Fasn) expression was also substantially elevated in *Fabp4*$^{-/-}$ macrophages and induced upon aP2-i treatment *in vivo* (data not shown). Collectively, these data indicate that aP2 action in macrophages is linked to the regulation of key enzymes involved in the *de novo* synthesis and desaturation of fatty acids.

To examine the impact of aP2-regulated SCD-1 activity in the resistance to ER stress in *Fabp4*$^{-/-}$ macrophages, we took two distinct but related approaches. First, we asked whether C16:1n7-palmitoleate, a product of *de novo* lipogenesis elevated in *Fabp4*$^{-/-}$ macrophages, could modify ER responses to lipids[34]. Strikingly, we found that WT macrophages pretreated with C16:1n7-palmitoleate became resistant to palmitate-induced ER stress and apoptosis but not to tunicamycin-induced ER stress, as determined by the P-PERK, P-eIF2–α cleaved PARP and *Ddit3* and s*Xbp1* levels (**Fig. 5d**,**e**). This pattern induced by C16:1n7-palmitoleate was highly reminiscent of genetic or chemical aP2 deficiency (**Fig. 5d**,**e**). Oleate, another fatty acid product of desaturation, which is not regulated to the same extent as palmitoleate in *Fabp4*$^{-/-}$ macrophages, could also protect against palmitate- or stearate-induced ER stress (**Supplementary Fig. 2b–d**).

Second, we used an siRNA-mediated approach to significantly deplete SCD-1 protein and activity in *Fabp4*$^{-/-}$ macrophages (**Fig. 5f**). Sensitivity to palmitate-induced ER stress and apoptosis

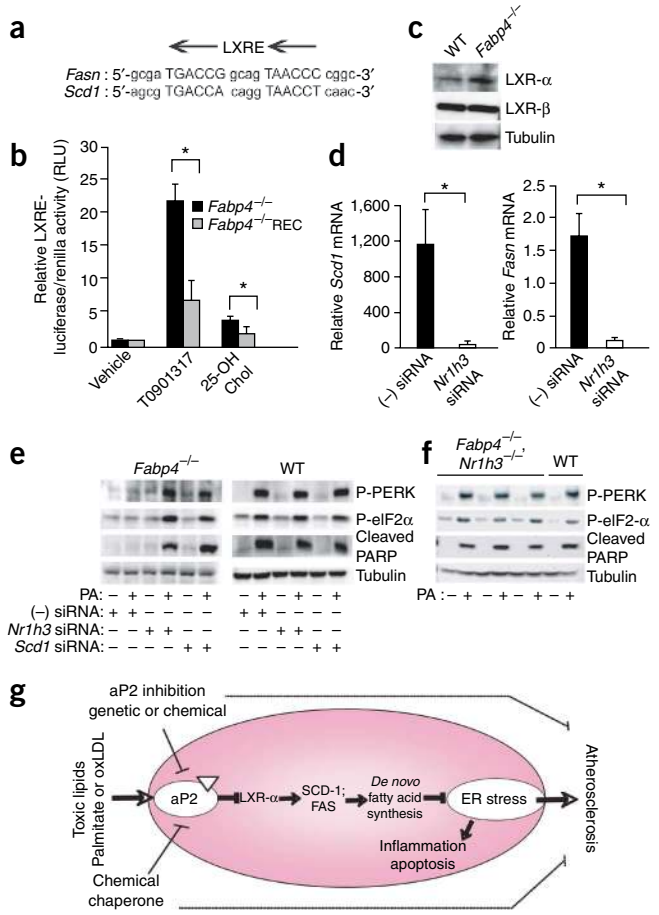

Figure 6 Linking toxic lipids to ER stress and atherosclerosis through aP2–LXR-α crosstalk. (**a**) Alignment of LXREs on *Fasn* and *Scd1* promoters. (**b**) LXR-driven transcriptional activity, as determined from various macrophage lines upon stimulation with a synthetic (T0901317, 10 μM) or endogenous (25-hydroxycholesterol, 10 μM) LXR ligand. Luciferase activity is reported after normalizing to transfection efficiency. (**c**) Relative LXR-α and LXR-β protein abundance in various macrophage lines, as examined by western blotting. (**d**) Relative *Scd1* and *Fasn* mRNA levels from *Fabp4*$^{-/-}$ macrophages treated with a scrambled (–) or *Nr1h3*-specific siRNA, as examined by qRT-PCR. (**e**) Western blotting for P-PERK and P-eIF2α in lysates from various macrophages treated with scrambled (–) siRNA or a specific siRNA against *Scd1* or *Nr1h3* and stressed with or without palmitate (500 μM). (**f**) Western blotting for P-PERK, P-eIF2-α and cleaved PARP in lysates from peritoneal macrophages from *Fabp4*$^{-/-}$;*Nr1h3*$^{-/-}$ or WT mice stressed with or without palmitate (500 μM). (**g**) A cellular lipotoxicity model. Toxic levels of lipids, such as palmitate or oxidized LDL (oxLDL), are sensed by the ER through an aP2-dependent pathway, induce the UPR and lead to macrophage apoptosis. The absence of aP2 serves to reactivate macrophage *de novo* lipogenesis pathways and promotes desaturation, particularly through LXR-α–mediated activation of SCD-1, leading to increased production of bioactive lipids and resistance to ER stress. Alleviation of macrophage ER stress, either through aP2 inhibition or enhancing ER function, is protective against atherosclerosis. Data represent means ± s.d.; $^{*}P < 0.05$.

was reestablished in the *Scd1*–specific siRNA–treated *Fabp4*$^{-/-}$ macrophages, but not in scrambled (control) siRNA–treated cells, as evidenced by increased P-PERK, P-eIF2-α, active caspase-3 and cleaved PARP levels (**Fig. 5g**). These results indicate that aP2-mediated regulation of SCD-1 activity is causally linked to lipid-induced ER stress responses in macrophages.

Unraveling the molecular mechanisms by which aP2 regulates SCD-1 is essential for understanding how lipid stress signals impinge on the lipid synthetic pathways. Both *Scd1* and *Fasn* are direct transcriptional targets of the nuclear receptor LXR (LXR-responsive elements, LXREs, are located on *Fasn*, between positions −669 and −665, and *Scd1*, between positions −1263 and −1248) (**Fig. 6a**)[35,36]. Thus, we analyzed whether LXR activity is altered in aP2-deficient macrophages by using an LXRE-driven reporter. The *Fabp4*$^{-/-}$ macrophages showed a marked elevation in stimulated LXR activity when compared to control *Fabp4*$^{-/-}$REC cells (**Fig. 6b**). These results indicate that aP2 negatively regulates LXR activity in WT macrophages. Consistently, we observed increased expression of LXR target genes *Abca1* (encoding ATP-binding cassette, sub-family A (ABC1), member 1), *Abcg1* (encoding ATP-binding cassette, sub-family G (WHITE), member 1) and *Cd5l* (encoding CD5 antigen–like) in *Fabp4*$^{-/-}$ macrophages (**Supplementary Fig. 4a–c**)[37–39]. Further examination revealed marked elevation of *Nr1h3* (LXR-α) mRNA and protein levels in the absence of aP2, whereas *Nr1h2* (LXR-β) expression remained unchanged between the genotypes (**Fig. 6c** and **Supplementary Fig. 4d,e**). Hence, the LXR-α expression seemed to be the main driver of the alterations seen in LXR target gene expression. To definitively link LXR-α activity to *Scd1* regulation, we next suppressed *Nr1h3* expression in *Fabp4*$^{-/-}$ macrophages using an siRNA-mediated knockdown approach (**Supplementary Fig. 5a**). Reduction of *Nr1h3* expression had only a partial effect on the expression genes regulated by both LXR-α and LXR-β, such as *Abca1* and *Abcg1*, but generated a profound effect on the expression of an LXR-α–exclusive target gene, *Cd5l* (**Supplementary Fig. 5b–d**)[37–39]. The reduction in LXR-α also led to substantial inhibition of both *Fasn* and *Scd1* mRNA levels, indicating that LXR-α is mainly responsible for the upregulation of these genes in the absence of aP2 (**Fig. 6d** and **Supplementary Fig. 5e**). Suppression of LXR-α also restored sensitivity to palmitate-induced ER stress and apoptosis, as determined by induction of P-PERK and P-eIF2-α and cleavage of PARP in *Fabp4*$^{-/-}$ macrophages (**Fig. 6e**). To validate these links in a genetic setting, we examined the lipid-induced ER stress response in primary peritoneal macrophages derived from mice with combined *Fabp4* and *Nr1h3* genetic deficiency. The expression of *Fasn* and *Scd1* was also markedly downregulated in *Fabp4*$^{-/-}$;*Nr1h3*$^{-/-}$ macrophages compared to *Fabp4*$^{-/-}$ cells (**Supplementary Fig. 6b,c**)[40]. The expression of CD5l was profoundly suppressed in double-mutant cells, whereas *Abca1* and *Abcg1* were only partially affected (**Supplementary Fig. 6d–f**)[37–39]. Consequently, the protection against palmitate-induced ER stress was also lost in the *Fabp4*$^{-/-}$;*Nr1h3*$^{-/-}$ cells, as determined by P-PERK, P-eIF2-α and PARP cleavage induction (**Fig. 6f**). Consistently, treatment of WT macrophages with a specific LXR agonist, T0901317, promoted resistance to lipid-induced ER stress, similar to aP2 deficiency (**Supplementary Fig. 5f**). These results illustrate that LXR-α is responsible for the upregulation of SCD-1 in the absence of aP2 and provides one crucial mechanism for how lipid stress signals may impinge on macrophage lipid metabolism and ER stress (**Fig. 6g**).

DISCUSSION

Macrophages are particularly vulnerable to lipid-induced toxicity and contribute to the pathogenesis of several metabolic derangements where exposure to lipids is increased, such as the foam cells in hypercholesterolemic atherosclerosis and adipose tissue–associated macrophages in obesity[2,10,41]. Previous studies have shown expression

of UPR markers in macrophages infiltrating the atherosclerotic lesions of both mice and humans[4,8]. These findings are complemented by *in vitro* studies demonstrating that accumulation of free cholesterol leads to apoptosis via activation of ER stress in macrophages[3]. Elevation of ER stress–associated macrophage apoptosis has been proposed to contribute to advanced atherosclerotic lesions in macrophages defective in insulin signaling[42]. Although these findings have sparked interest, demonstration of a link between macrophage ER stress and atherogenesis *in vivo* and the mechanisms integrating lipid signals to ER function in macrophages has been challenging. Hence, modulation of ER stress, especially upstream of the apoptotic execution pathways, becomes crucial in understanding the extent of its contribution to the pathogenesis of atherosclerosis. Our data provide insight into these key questions. First, we show that the lipid chaperone aP2 is an obligatory mediator coupling toxic lipids to ER stress in macrophages *in vitro* and *in vivo*. Second, we show that alleviating ER stress, either by the use of a chemical chaperone or through the inhibition of a lipid chaperone, provides marked protection against macrophage ER stress, cell death and atherosclerosis.

The unexpected and striking upregulation of aP2 by saturated fatty acids and downregulation by PBA in macrophages led to the uncovering of a previously unknown function of the lipid chaperones in mitigating ER stress in macrophages *in vitro* and in atherosclerotic lesions *in vivo*. The observations place aP2 as a central modulator of lipid-induced ER stress responses—a process for which there had previously been little mechanistic insight. It is also established that the role of macrophage aP2 action on atherosclerosis is not related to other metabolic alterations, such as changes in insulin sensitivity or dyslipidemia, and is therefore intrinsic to macrophages[22,43]. Similarly, treatment with the PBA doses used in this study, as reported earlier, does not yield substantial metabolic alterations[7]. Therefore, our present findings unravel a mechanism by which aP2 might mediate its antiatherosclerotic effects through modulating the UPR, helping to clarify a much sought after but very challenging aspect of lipid chaperone biology in macrophages and in atherosclerosis[4,8]. Finally, our findings offer tools to modulate ER stress responses associated with dyslipidemia *in vitro* and *in vivo* that may facilitate therapeutic applications, including that of aP2.

Marked resistance to ER stress can be achieved by blocking aP2 action, which is dependent on SCD-1 activity. aP2 prevents enrichment of macrophages in desaturation products such as C16:1n7-palmitoleate, a molecule that provides relief from lipid-induced ER stress, in addition to its other reported beneficial endocrine effects[34]. It will be useful to determine whether C16:1n7 supplementation or a diet enriched with palmitoleate can confer resistance to macrophage ER stress and reduction in atherosclerosis in future studies. In this study, we showed that enhanced LXR-α activity in *Fabp4*$^{-/-}$ macrophages drives *Fasn* and *Scd1* transcription and resistance to lipotoxic ER stress and identified the transcriptional mechanism underlying this function of aP2. Although we have shown that aP2 inhibits LXR-α expression, the mechanisms by which aP2 regulates LXR-α activity is not completely illuminated. Nevertheless, these observations raise the possibility of a specific link between the nuclear hormone receptor LXR-α and ER stress responses. Overall, this study shows that *de novo* fatty acid synthesis and desaturation can be highly beneficial, if not essential, for defending ER function when macrophages are exposed to toxic lipids. Accordingly, although SCD-1 expression is elevated in the obese liver, inhibition of SCD-1 in the whole body may not have great therapeutic prospects in diabetes, owing to adverse metabolic effects seen in the macrophages and pancreatic β cells[10,44]. Indeed, systemic inhibition of SCD-1 leads to severe atherosclerosis, despite protection from obesity and hepatosteatosis[45]. Similarly, activation of LXR in the whole body leads to undesirable metabolic side effects, particularly in the liver. In contrast, selective upregulation of LXR and SCD-1 activity in macrophages and adipocytes and downregulation in liver may be an optimal strategy and yield the most beneficial overall metabolic outcome, including protection against diabetes and atherosclerosis[29].

It is noteworthy that our findings do not exclude other LXR-regulated macrophage responses as additional contributors to the impact of aP2 on macrophage function and atherosclerosis. Because the most marked upregulation seen in the *Fabp4*$^{-/-}$ macrophages is that of *Scd1* and *CD5L* genes, and knocking down SCD-1 alone is sufficient to reestablish sensitivity to lipid-induced ER dysfunction in the *Fabp4*$^{-/-}$ macrophages, LXR-mediated lipogenesis pathways are likely to dominate the aP2-deficient phenotype related to lipotoxic ER stress. Yet, the impact of aP2, directly or through the regulation of LXR or PPAR, on inflammatory functions of macrophages may also have a role in preventing atherosclerosis[31]. aP2 expression is limited to macrophages and dendritic cells in normal conditions as well as in atherosclerotic lesions (**Fig. 2b** and data not shown)[10,22,46,47]. Although aP2 does not alter antigen presentation, studies have shown that it can affect T cell priming and cytokine production[19,46,47]. Moreover, ER stress responses and inflammation are integrated at several levels and modulate each other; inflammation can compromise ER function, and ER stress can promote inflammation[10]. The links between inflammatory pathways and ER stress are of great interest in chronic metabolic disease, and understanding the intricate links between lipid metabolism and the immune system and identification of molecular targets like aP2 at this interface are crucial for developing effective therapeutics against the metabolic disease cluster.

In conclusion, we have uncovered a previously unknown function for aP2 in lipid-induced ER stress signaling in macrophages, while addressing the essential role of ER stress in vascular disease progression (**Fig. 6g**). The ability to defend against the lipids disrupting ER function illustrates a unique metabolic adaptation capacity of macrophages that is governed by the lipid chaperones. aP2 in particular, and perhaps cytosolic lipid chaperones in general, could function as a molecular sensor for fatty acids and as a central coordinator of metabolic ER stress. Because aP2 deficiency can alleviate the ER stress that occurs during atherosclerosis, similar to the actions of a chemical chaperone, our findings offer insights into the detrimental role of macrophage ER stress in atherosclerosis and the benefits of addressing this target to treat cardiovascular disease.

METHODS

Methods and any associated references are available in the online version of the paper at http://www.nature.com/naturemedicine/.

Note: Supplementary information is available on the Nature Medicine website.

ACKNOWLEDGMENTS

This project has been supported by grants from the US National Institutes of Health DK DK52539 (to G.S.H.), HL65405 (to M.F.L. and G.S.H.) and DK59637 (Lipid, Lipoprotein and Atherosclerosis Core of the Vanderbilt Mouse Metabolic Phenotype Center). E.E. is supported by the Ruth Kirschstein National Research Award (F32 HL090258). We are grateful to the members of the Hotamisligil lab, J. Chen and R. Bachman for their scientific input and contributions, to A. Onur for technical assistance, to R. Foote and K. Gilbert for administrative support, to D. Mangelsdorf (University of Texas Southwestern) for TK-LXRE-X3luc reporter and *Nr1h3*$^{-/-}$ mice, and A. Edgar (Fournier) for the ACAT inhibitor. The pGEX-aP2-LM (R126L, Y128F) plasmid was a generous gift from D. Bernlohr (University of Minnesota).

AUTHOR CONTRIBUTIONS

E.E. developed the hypothesis, designed and performed the bulk of the experiments, analyzed all data and wrote the manuscript; V.R.B. contributed to the *in vivo* studies; J.R.M. contributed to the *in vitro* studies and conducted data analysis, K.N.C. and M.E.S. contributed to the *in vitro* studies; L.M., M.M.W. and S.M.W. contributed to the analysis of lipidomic data; S.F. and M.F.L. contributed to the analysis of *in vivo* data and assisted with writing; and G.S.H. developed the hypothesis, designed and analyzed all data, wrote the manuscript and supervised the project and the peer review process.

COMPETING INTERESTS STATEMENT

The authors declare competing financial interests: details accompany the full-text HTML version of the paper at http://www.nature.com/naturemedicine/.

Published online at http://www.nature.com/naturemedicine/.
Reprints and permissions information is available online at http://npg.nature.com/reprintsandpermissions/.

1. Hotamisligil, G.S. Inflammation and metabolic disorders. *Nature* **444**, 860–867 (2006).
2. Gregor, M.F. & Hotamisligil, G.S. Thematic review series: Adipocyte Biology. Adipocyte stress: the endoplasmic reticulum and metabolic disease. *J. Lipid Res.* **48**, 1905–1914 (2007).
3. Feng, B. *et al.* The endoplasmic reticulum is the site of cholesterol-induced cytotoxicity in macrophages. *Nat. Cell Biol.* **5**, 781–792 (2003).
4. Tabas, I. Consequences and therapeutic implications of macrophage apoptosis in atherosclerosis: the importance of lesion stage and phagocytic efficiency. *Arterioscler. Thromb. Vasc. Biol.* **25**, 2255–2264 (2005).
5. Ozcan, U. *et al.* Endoplasmic reticulum stress links obesity, insulin action and type 2 diabetes. *Science* **306**, 457–461 (2004).
6. Ozawa, K. *et al.* The endoplasmic reticulum chaperone improves insulin resistance in type 2 diabetes. *Diabetes* **54**, 657–663 (2005).
7. Ozcan, U. *et al.* Chemical chaperones reduce ER stress and restore glucose homeostasis in a mouse model of type 2 diabetes. *Science* **313**, 1137–1140 (2006).
8. Myoishi, M. *et al.* Increased endoplasmic reticulum stress in atherosclerotic plaques associated with acute coronary syndrome. *Circulation* **116**, 1226–1233 (2007).
9. Ron, D. & Walter, P. Signal integration in the endoplasmic reticulum unfolded protein response. *Nat. Rev. Mol. Cell Biol.* **8**, 519–529 (2007).
10. Hotamisligil, G.S. & Erbay, E. Nutrient sensing and inflammation in metabolic diseases. *Nat. Rev. Immunol.* **8**, 923–934 (2008).
11. Sriburi, R., Jackowski, S., Mori, K. & Brewer, J.W. XBP1: a link between the unfolded protein response, lipid biosynthesis, and biogenesis of the endoplasmic reticulum. *J. Cell Biol.* **167**, 35–41 (2004).
12. Brookheart, R.T., Michel, C.I. & Schaffer, J.E. As a matter of fat. *Cell Metab.* **10**, 9–12 (2009).
13. Ferré, P. & Foufelle, F. SREBP-1c transcription factor and lipid homeostasis: clinical perspective. *Horm. Res.* **68**, 72–82 (2007).
14. Oyadomari, S., Harding, H.P., Zhang, Y., Oyadomari, M. & Ron, D. Dephosphorylation of translation initiation factor 2α enhances glucose tolerance and attenuates hepatosteatosis in mice. *Cell Metab.* **7**, 520–532 (2008).
15. Rutkowski, D.T. *et al.* UPR pathways combine to prevent hepatic steatosis caused by ER stress–mediated suppression of transcriptional master regulators. *Dev. Cell* **15**, 829–840 (2008).
16. Ramanadham, S. *et al.* Apoptosis of insulin-secreting cells induced by endoplasmic reticulum stress is amplified by overexpression of group VIA calcium–independent phospholipase A2 (iPLA2 β) and suppressed by inhibition of iPLA2 β. *Biochemistry* **43**, 918–930 (2004).
17. Tessitore, A. *et al.* GM1-ganglioside–mediated activation of the unfolded protein response causes neuronal death in a neurodegenerative gangliosidosis. *Mol. Cell* **15**, 753–766 (2004).
18. Furuhashi, M. & Hotamisligil, G.S. Fatty acid–binding proteins: role in metabolic diseases and potential as drug targets. *Nat. Rev. Drug Discov.* **7**, 489–503 (2008).
19. Shum, B.O. *et al.* The adipocyte fatty acid–binding protein aP2 is required in allergic airway inflammation. *J. Clin. Invest.* **116**, 2183–2192 (2006).
20. Hotamisligil, G.S. *et al.* Uncoupling of obesity from insulin resistance through a targeted mutation in aP2, the adipocyte fatty acid binding protein. *Science* **274**, 1377–1379 (1996).
21. Uysal, K.T., Scheja, L., Wiesbrock, S.M., Bonner-Weir, S. & Hotamisligil, G.S. Improved glucose and lipid metabolism in genetically obese mice lacking aP2. *Endocrinology* **141**, 3388–3396 (2000).
22. Makowski, L. *et al.* Lack of macrophage fatty-acid–binding protein aP2 protects mice deficient in apolipoprotein E against atherosclerosis. *Nat. Med.* **7**, 699–705 (2001).
23. Cao, H. *et al.* Regulation of metabolic responses by adipocyte/macrophage fatty acid–binding proteins in leptin-deficient mice. *Diabetes* **55**, 1915–1922 (2006).
24. Ozcan, U. *et al.* Loss of the tuberous sclerosis complex tumor suppressors triggers the unfolded protein response to regulate insulin signaling and apoptosis. *Mol. Cell* **29**, 541–551 (2008).
25. Borradaile, N.M. *et al.* Disruption of endoplasmic reticulum structure and integrity in lipotoxic cell death. *J. Lipid Res.* **47**, 2726–2737 (2006).
26. Lai, E., Bikopoulos, G., Wheeler, M.B., Rozakis-Adcock, M. & Volchuk, A. Differential activation of ER stress and apoptosis in response to chronically elevated free fatty acids in pancreatic beta-cells. *Am. J. Physiol. Endocrinol. Metab.* **294**, E540–E550 (2008).
27. Schaffer, J.E. Lipotoxicity: when tissues overeat. *Curr. Opin. Lipidol.* **14**, 281–287 (2003).
28. Tuncman, G. *et al.* A genetic variant at the fatty acid–binding protein aP2 locus reduces the risk for hypertriglyceridemia, type 2 diabetes and cardiovascular disease. *Proc. Natl. Acad. Sci. USA* **103**, 6970–6975 (2006).
29. Furuhashi, M. *et al.* Treatment of diabetes and atherosclerosis by inhibiting fatty-acid–binding protein aP2. *Nature* **447**, 959–965 (2007).
30. Sha, R.S., Kane, C.D., Xu, Z., Banaszak, L.J. & Bernlohr, D.A. Modulation of ligand binding affinity of the adipocyte lipid-binding protein by selective mutation. Analysis in vitro and in situ. *J. Biol. Chem.* **268**, 7885–7892 (1993).
31. Makowski, L., Brittingham, K.C., Reynolds, J.M., Suttles, J. & Hotamisligil, G.S. The fatty acid-binding protein, aP2, coordinates macrophage cholesterol trafficking and inflammatory activity. Macrophage expression of aP2 impacts peroxisome proliferator-activated receptor γ and IκB kinase activities. *J. Biol. Chem.* **280**, 12888–12895 (2005).
32. Enoch, H.G., Catala, A. & Strittmatter, P. Mechanism of rat liver microsomal stearyl-CoA desaturase. Studies of the substrate specificity, enzyme-substrate interactions, and the function of lipid. *J. Biol. Chem.* **251**, 5095–5103 (1976).
33. Heinemann, F.S. & Ozols, J. Stearoyl-CoA desaturase, a short-lived protein of endoplasmic reticulum with multiple control mechanisms. *Prostaglandins Leukot. Essent. Fatty Acids* **68**, 123–133 (2003).
34. Cao, H. *et al.* Identification of a lipokine, a lipid hormone linking adipose tissue to systemic metabolism. *Cell* **134**, 933–944 (2008).
35. Joseph, S.B. *et al.* Direct and indirect mechanisms for regulation of fatty acid synthase gene expression by liver X receptors. *J. Biol. Chem.* **277**, 11019–11025 (2002).
36. Chu, K., Miyazaki, M., Man, W.C. & Ntambi, J.M. Stearoyl-coenzyme A desaturase 1 deficiency protects against hypertriglyceridemia and increases plasma high-density lipoprotein cholesterol induced by liver X receptor activation. *Mol. Cell. Biol.* **26**, 6786–6798 (2006).
37. Venkateswaran, A. *et al.* Human white/murine ABC8 mRNA levels are highly induced in lipid-loaded macrophages. A transcriptional role for specific oxysterols. *J. Biol. Chem.* **275**, 14700–14707 (2000).
38. Repa, J.J. *et al.* Regulation of absorption and ABC1-mediated efflux of cholesterol by RXR heterodimers. *Science* **289**, 1524–1529 (2000).
39. Joseph, S.B. *et al.* LXR-dependent gene expression is important for macrophage survival and the innate immune response. *Cell* **119**, 299–309 (2004).
40. Peet, D.J. *et al.* Cholesterol and bile acid metabolism are impaired in mice lacking the nuclear oxysterol receptor LXR alpha. *Cell* **93**, 693–704 (1998).
41. Aqel, N.M., Ball, R.Y., Waldmann, H. & Mitchinson, M.J. Monocytic origin of foam cells in human atherosclerotic plaques. *Atherosclerosis* **53**, 265–271 (1984).
42. Han, S. *et al.* Macrophage insulin receptor deficiency increases ER stress-induced apoptosis and necrotic core formation in advanced atherosclerotic lesions. *Cell Metab.* **3**, 257–266 (2006).
43. Boord, J.B. *et al.* Adipocyte fatty acid–binding protein, aP2, alters late atherosclerotic lesion formation in severe hypercholesterolemia. *Arterioscler. Thromb. Vasc. Biol.* **22**, 1686–1691 (2002).
44. Listenberger, L.L. *et al.* Triglyceride accumulation protects against fatty acid–induced lipotoxicity. *Proc. Natl. Acad. Sci. USA* **100**, 3077–3082 (2003).
45. Brown, J.M. *et al.* Inhibition of stearoyl-coenzyme A desaturase 1 dissociates insulin resistance and obesity from atherosclerosis. *Circulation* **118**, 1467–1475 (2008).
46. Rolph, M.S. *et al.* Regulation of dendritic cell function and T cell priming by the fatty acid–binding protein aP2. *J. Immunol.* **177**, 7794–7801 (2006).
47. Erbay, E., Cao, H. & Hotamisligil, G.S. Adipocyte/macrophage fatty acid binding proteins in metabolic syndrome. *Curr. Atheroscler. Rep.* **9**, 222–229 (2007).

ONLINE METHODS

Mice, immunhistochemistry and quantification of arterial lesions. We established colonies for *Fabp4*$^{-/-}$;*Apoe*$^{-/-}$, *Apoe*$^{-/-}$ and *Fabp4*$^{-/-}$;*Nr1h3*$^{-/-}$ mice on the C57BL/6 background. *Nr1h3*$^{-/-}$ mice used in this study were previously published[40]. The Harvard Medical Area Standing Committee on Animals approved the mouse handling procedures. We fed mice with Western diet for 16 weeks as previously described[29]. After killing them, we flushed their aortas through the left ventricle and dissected them as described previously[29]. To detect macrophages in arterial lesions, we fixed 5-μm serial cryosections of the proximal aorta in acetone and incubated them with antibodies following the manufacturer's recommendations and previously established protocols[48]. We incubated the sections with biotinylated secondary antibodies and then with alkaline phosphatase–labeled avidin–conjugated antibodies using an ABC kit (Vector Lab). We quantified lesion areas with Imaging System KS 300 (2.0; Kontron Electronik GmbH). For immunofluorescence stainings, we applied Alexa Fluor 488– and Alexa Fluor 647–conjugated secondary antibodies after an overnight incubation of the lesions with the primary antibody. The primary antibodies used were specific for P-eIF2α (Invitrogen), ATF-3 (Santa Cruz) and MOMA-2 (Accurate Chemical & Scientific Corp.). We used DAPI for counterstaining. We measured the mean fluorescence intensity for each ER stress marker in the macrophage-dense areas using Auxiovision 4.6 software ($n \geq 3$). For TUNEL analysis, we pretreated the serial sections with 3% citric acid, fixed them in 4% paraformaldehyde and stained them with an *in situ* cell death detection alkaline phosphatase kit (Roche). After visualization of alkaline phosphatase with Fast Red TR/Naphthol AS-NX substrate (Sigma), we counted TUNEL-positive cells ($n = 18$ per aorta).

Analysis of serum lipids. We fasted mice were fasted (4 h) and measured the serum cholesterol and triglyceride concentrations by conventional enzymatic methods using reagents from Raichem and SoftMax Pro5 software (Molecular Devices).

Quantitative real-time PCR and immunoblot analysis. We isolated RNA from macrophages with the RNeasy kit (Qiagen). We synthesized complementary DNA with iScript (Biorad), and we performed qRT-PCR with an ABI Thermocycler. We collected macrophage proteins and assessed total protein content as previously described[31]. We subjected equal amounts of total protein per sample to SDS-PAGE and performed western blotting as described previously[29,31].

Cell culture, knockdown, TUNEL caspase and reporter assays. Unless otherwise indicated, we used bone marrow–derived mouse macrophage lines. We carried out reconstitution experiments in bone marrow–derived macrophages that were immortalized[29]. When indicated in the text or in **Figures 5c** and **6f**, we used peritoneal macrophages derived by 4% thioglycolate elicitation. We maintained macrophages in RPMI supplemented with 10% FBS. For caspase-3 and caspase-7 activity assays, we plated cells on 96-well plates, and when they reached confluency, we treated them with the appropriate reagents, such as fatty acids (Sigma) or acetylated LDL (Biomedical Technologies) along with ACAT inhibitor (Fournier) to activate caspase activity over a time course. We measured caspase-3 and caspase-7 activity with the caspase 3/7-Glo kit (Promega) according to the manufacturer's instructions. For loss-of-function experiments, we transfected siRNAs (Ambion) into 80% confluent macrophages with siImporter (Upstate) according to the manufacturer's instructions. Primer sequences for *Fabp4*, *Ddit3*, *Fasn*, *Scd1*, s*Xbp1*, *Abca1*, *Abcg1* and *Cd5l* have been previously published[49–51]. All primers used for qRT-PCR were synthesized at Qiagen and for siRNA at Ambion. The pGEX-aP2-LM (R126L, Y128F) plasmid was a generous gift from D. Bernlohr and was recloned into a pCDNA3 vector[4]. The siRNA sequences for *Scd1* were sense: 5′-GCCUUUAAUCAACCCAA GATT-3′ and antisense: 5′-UCUUGGGUUGAUUAAA-GGCTT-3′ and for *Nr1h3* were sense: 5′-GGACUUCAGUUACAACCGGTT-3′ and antisense: 5′-CCGGUUGUAACUGAAGUC-CTT-3′. For reporter assays, we plated macrophages on 12-well plates, grew them to 80% confluency and transfected them with the appropriate plasmids using Superfect (Qiagen). Twenty-four hours after transfection, we treated cells with LXR ligands T0901317 (10 μM) and 25 hydroxy cholesterol (10 μM) (Sigma) or DMSO followed by luciferase assays using the Dual-Luciferase assay system (Promega) according to the manufacturer's instructions.

Lipidomics. Fatty acids concentrations in one experiment ($n = 5$) were measured by Lipomics, Inc. in each neutral lipid class cholesterol esters, diacylglycerol, phospholipids, FFAs and triglycerides. We extracted the lipids from plasma and tissues in the presence of authentic internal standards a previously described method[34] using chloroform mixed with methanol (2:1 vol/vol). We separated individual lipid classes within each extract by liquid chromatography (Agilent Technologies model 1100 Series)[34]. We transesterified each lipid class in 1% sulfuric acid in methanol in a sealed vial under a nitrogen atmosphere at 100 °C for 45 min. We extracted the resulting fatty acid methyl esters from the mixture with hexane containing 0.05% butylated hydroxytoluene and prepared them for gas chromatography by sealing the hexane extracts under nitrogen. We separated fatty acid methyl esters and quantified them by capillary gas chromatography (Agilent Technologies 6890) equipped with a 30-m DB-88MS capillary column (Agilent Technologies) and a flame-ionization detector.

Statistical analyses. We used one-way ANOVA to determine significance in lesion size differences. For TUNEL assays, we determined statistical differences by one-way ANOVA multiple comparisons versus the control group (Dunn's method) in **Figure 1** and the statistical differences in mean of TUNEL^{+}/MOMA-2^{+} lesion area between the groups by the Mann-Whitney rank-sum test in **Figure 3**. For lipidomic analyses, we examined the distributions of each fatty acid within each lipid class for extreme outliers or poor measurement[52,53]. If a fatty acid was missing more than 30% of its observations, we removed it from further analysis. Initial statistical analysis included a one-way ANOVA to identify fatty acids within each lipid class that differed between the genotypes. We visualized the results of the one-way ANOVA by lipid class composition analysis. We made direct comparisons between groups using a Wilcoxon rank test and visualized them with bar plots.

48. Gregor, M.F. *et al.* Endoplasmic reticulum stress is reduced in tissues of obese subjects after weight loss. *Diabetes* **58**, 693–700 (2009).
49. Joseph, S.B. *et al.* LXR-dependent gene expression is important for macrophage survival and the innate immune response. *Cell* **119**, 299–309 (2004).
50. Furuhashi, M. *et al.* Treatment of diabetes and atherosclerosis by inhibiting fatty-acid-binding protein aP2. *Nature* **447**, 959–965 (2007).
51. Venkateswaran, A. *et al.* Human white/murine ABC8 mRNA levels are highly induced in lipid-loaded macrophages. A transcriptional role for oxysterols. *J. Biol. Chem.* **275**, 14700–14707 (2000).
52. Pan, W. On the use of permutation in and the performance of a class of nonparametric methods to detect differential gene expression. *Bioinformatics* **19**, 1333–1340 (2003).
53. Kuehl, R.O. *Design of Experiments: Statistical Principles of Research Design and Analysis*. 2nd edn., 56–58 (Duxbury Press, Pacific Grove, California, 2000).

doi:10.1038/nm.2067

Corrigendum: Neuronal PTP1B regulates body weight, adiposity and leptin action

Kendra K Bence, Mirela Delibegovic, Bingzhong Xue, Cem Z Gorgun, Gokhan S Hotamisligil, Benjamin G Neel & Barbara B Kahn
***Nat. Med.* 12, 917–924 (2006); published online 16 July 2006; corrected after print 7 January 2010**

In the version of this article initially published, the source of the Nestin-Cre mice was incorrectly stated as Jackson Labs. The correct source of the Nestin-Cre mice (which were on a mixed 129/Sv × C57BL/6 hybrid background) was R. Klein (Max Planck Institute of Neurobiology). The error has been corrected in the HTML and PDF versions of the article.

Addendum: Neuronal PTP1B regulates body weight, adiposity and leptin action

Kendra K Bence, Mirela Delibegovic, Bingzhong Xue, Cem Z Gorgun, Gokhan S Hotamisligil, Benjamin G Neel & Barbara B Kahn
***Nat. Med.* 12, 917–924 (2006); published online 16 July 2006; corrected after print 7 January 2010; addendum published after print 7 January 2010**

The widespread use of Nestin-Cre mice has led to an increasing awareness of potential diet- and strain-dependent differences in body weight in these mice. Accordingly, we have tested the effect of Nestin-Cre alone in several strains of mice and have observed marked differences in body weight between Nestin-Cre and wild-type mice fed chow in some, but not all, strains (data not shown). Given these strain differences, and to rule out potential spurious results, we would like to add additional control data from experiments performed at the time of the original studies in our paper showing no effect of Nestin-Cre expression alone on body weight (**Fig. 1**).

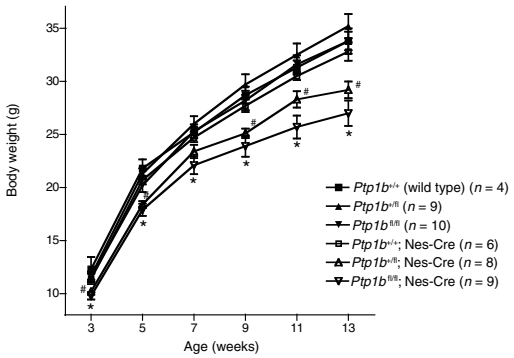

Figure 1 Body weight curves of male mice fed a high-fat diet from weaning (3 weeks of age). *Ptp1b*$^{+/fl}$ Nes-Cre and *Ptp1b*$^{fl/fl}$ Nes-Cre mice weighed significantly less than *Ptp1b*$^{+/+}$ Nes-Cre mice by two-way ANOVA with repeated measures ($P = 0.013$ and $P = 0.003$, respectively); #$P < 0.05$ *Ptp1b*$^{+/fl}$ Nes-Cre versus *Ptp1b*$^{+/+}$ Nes-Cre, and *$P < 0.05$ *Ptp1b*$^{fl/fl}$ Nes-Cre versus *Ptp1b*$^{+/+}$ Nes-Cre by unpaired two-tailed Student's *t* test at the indicated time points. Body weights were not different between *Ptp1b*$^{+/+}$ Nes-Cre mice and *Ptp1b*$^{+/+}$ (wild-type), *Ptp1b*$^{+/fl}$ or *Ptp1b*$^{fl/fl}$ mice fed a high-fat diet from weaning (by two-way ANOVA with repeated measures or two-tailed Student's *t* test). All mice were on a mixed 129/Sv × C57BL/6 hybrid background.

Erratum: Reducing endoplasmic reticulum stress through a macrophage lipid chaperone alleviates atherosclerosis

Ebru Erbay, Vladimir R Babaev, Jared R Mayers, Liza Makowski, Khanichi N Charles, Melinda E Snitow, Sergio Fazio, Michelle M Wiest, Steven M Watkins, MacRae F Linton & Gökhan S Hotamisligil
***Nat. Med.* 15, 1383–1391 (2009); published online 29 November 2009; corrected after print 4 February 2010**

In the version of this article initially published, the official symbol for the gene encoding the aP2 protein was misidentified as *Tcfap2a* (the gene symbol for the transcription factor AP-2). The correct gene symbol is *Fabp4*. In no instances anywhere in the study was AP-2 examined. Additionally, Supplementary Figure 2a should also have been cited where Figure 2c was cited. The errors have been corrected in the HTML and PDF versions of the article.